Variability of the tropical and subtropical ocean surface latent heat flux during 1989–2000

Jiping Liu[1] and Judith A. Curry[1]

Received 29 September 2005; revised 17 January 2006; accepted 31 January 2006; published 7 March 2006.

[1] We assess the consistencies and discrepancies of the interannual variability and decadal trend of the ocean surface latent heat flux (LHF) for the period 1989–2000 among two satellite-based data sets and two reanalysis products over the tropics and subtropics. The data sets show encouraging agreement on the spatial/temporal variations of the LHF, particularly during 1992–1997, but some discrepancies are noticed. These discrepancies are primarily caused by the differences of the input meteorological state variables used to calculate LHF, particularly for the air specific humidity. Both the satellite-based data sets and reanalysis products show a statistically significant decadal-scale positive trend in the LHF, which is independent of the El Niño-Southern Oscillation, with the strongest trends in the subtropical Southeast Pacific and Southeast Indian Ocean. This trend in the LHF is associated primarily with an increasing trend of the surface wind speed. **Citation:** Liu, J., and J. A. Curry (2006), Variability of the tropical and subtropical ocean surface latent heat flux during 1989–2000, *Geophys. Res. Lett.*, *33*, L05706, doi:10.1029/2005GL024809.

1. Introduction

[2] The ocean surface latent heat flux (LHF) plays a critical role in understanding and modeling the exchange of heat and moisture between the atmosphere and ocean. The LHF is the second largest component of the ocean surface heat budget, and an important component of the atmospheric hydrological cycle. The variability of the net surface heat flux on timescales exceeding the diurnal is dominated by the variability of the LHF [e.g., *da Silva et al.*, 1994; *Chou et al.*, 2004]. The LHF, which is directly related to the ocean surface evaporative flux, also plays a key role in the salinity budget of the upper ocean. Accurate ocean surface latent heat flux data sets are essential for understanding air-sea interactions on a variety of scales, forcing ocean models, evaluating numerical weather prediction and coupled climate models, and understanding the ocean heat and fresh water budget [e.g., *Working Group on Air-Sea Fluxes* (*WGASF*), 2001; *Curry et al.*, 2004].

[3] The Comprehensive Ocean-Atmosphere Data Set (COADS) has the most complete surface marine observations since 1854, obtained mainly from merchant ships [*Woodruff et al.*, 1993]. Although the COADS-based fluxes are the generally accepted climatology, they suffer serious spatial and temporal sampling problems and measurement uncertainties [e.g., *da Silva et al.*, 1994; *Chou et al.*, 2004]. Therefore, it is desirable to construct a reliable long-term data set of the ocean surface latent heat flux with global sampling and temporal scale on the order of days. Recently, several satellite data analyses and numerical weather prediction (NWP) reanalysis projects have produced new versions of the LHF data sets at the desired space/time resolution and coverage. Comparisons of the original versions of these LHF data sets [e.g., *Kubota et al.*, 2003] showed substantial discrepancies in the zonally-averaged LHF values, particularly for the tropics and subtropics.

[4] There is considerable emerging interest to use these LHF data sets to analyze interannual variability [e.g., *WGASF*, 2001]. Extensive investigation of the bias and random errors in these data sets is being conducted by the SEAFLUX project [*Curry et al.*, 2004], which has motivated improvements to the satellite-based flux products. Bias errors in these data sets would not, by themselves, preclude using these data sets to investigate interannual variability and trends. A key issue in such applications is to identify and understand any spurious spikes and trends associated discontinuities in the satellite data sets (i.e., drift, discontinuities between subsequent satellites, contamination from volcanic eruptions) that are used as input meteorological state variables for the satellite-based flux products and also used in the NWP reanalyses (through data assimilation and specification of the state of the sea surface boundary).

[5] In this study, we examine the ocean surface latent heat flux from recent satellite-based data sets and NWP reanalysis products, with focus on the period 1989-2000 for the tropics and subtropics. We assess the consistencies and discrepancies among these LHF data sets, identify the LHF trend, and discuss relative impact of the El Niño-Southern Oscillation (ENSO) on the identified LHF trend.

2. Data

[6] We utilize four different data sets of the ocean surface latent heat flux, including two satellite-based data sets and two NWP reanalysis products. The time period selected for this study is 1989–2000, which makes use of the current generation of passive microwave radiometers (SSM/I, a critical element in the satellite-based data sets). Our analysis focuses on the tropical and subtropical oceans (35°S–35°N), where the signal from interannual variability is expected to the strongest.

[7] The two satellite-based data sets of the ocean surface latent heat flux are the Goddard Satellite-Based Surface Turbulent Fluxes Version 2 (GSSTF2) and the Hamburg Ocean-Atmosphere Parameters and Fluxes Version 2 (HOAPS2). The GSSTF2 data set with filled missing values [*Chou et al.*, 2004; *Romanou et al.*, 2006] has a spatial

[1]School of Earth and Atmospheric Sciences, Georgia Institute of Technology, Atlanta, Georgia, USA.

0094-8276/06/2005GL024809$05.00

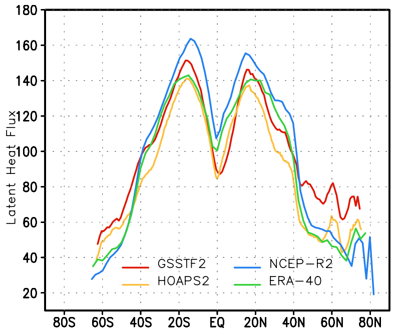

Figure 1. Zonally-averaged annual mean LHF (W/m^2) over the period 1989–2000.

resolution of 1° degree for the period January 1989–December 2000 and a temporal resolution of one day. The HOAPS2 data set [*Grassl et al.*, 2000] covers the period January 1988–December 2002 with 0.5° degree spatial resolution and pentad temporal resolution.

[8] The National Center for Environmental Prediction (NCEP) and European Centre for Medium-Range Weather Forecast (ECMWF) reanalysis products use state-of-the-art global data assimilation techniques and observational data from a variety of sources to generate long-term data sets (*Kanamitsu et al.* [2002], http://www.ecmwf.int/research/era). The NCEP Reanalysis II (NCEP-R2) provides data at a spatial resolution of T62 (~1.9° degree) from 1979 to present. The ECMWF 40-Year Reanalysis (ERA-40) provides data at a spatial resolution of 2.5° degree from January 1958 to August 2002.

[9] Values of the ocean surface latent heat flux in each of the four data sets are derived using bulk aerodynamic flux formulae of the form $LHF = \rho_a L_v C_E U(q_s - q_a)$, where ρ_a is the density of air, L_v is the latent heat of vaporization, C_E is the turbulent exchange coefficient, U is the near surface wind speed, q_s is the saturated specific humidity as a function of sea surface temperature (SST), and q_a is the near surface air specific humidity. The bulk formula links the LHF to mean values of sea surface temperature, wind speed and air specific humidity averaged over the timescale of turbulent eddies. The four data sets differ in their determination of the ocean surface latent flux through the use of different sources for the three input meteorological state variables and different bulk flux algorithms.

3. Comparisons of the Four Data Sets

[10] Figure 1 shows the zonally-averaged ocean surface latent heat flux for each of the four data sets (new versions). For comparisons, also see the zonally-averaged LHF values for the original versions of these data sets as reported by *Kubota et al.* [2003, Figure 5a]. The original versions of these data sets showed extremely large discrepancies among the zonally-averaged LHF values, which are as large as ~40–60% in the tropics and ~25–45% in the subtropics of the mean values of the four data sets there. By contrast, the new versions of these data sets (the versions used in this paper) show that discrepancies among the data sets is approximately half that seen in the original versions of these data sets. Improvements to the new versions of the satellite-based data sets include use of improved data sets for the input variables and improved bulk flux algorithms. Overall improvements to the new versions of the NWP reanalysis products are summarized by *Kanamitsu et al.* [2002] and by ECMWF (http://www.ecmwf.int/research/era).

[11] Figure 2a shows the anomaly time series of the monthly averaged LHF over the tropical and subtropical oceans. In general, all data sets show similar temporal variations, and the range of the LHF values between the various data sets is generally smaller than the magnitude of their variability for most of the time period, particularly from 1992 to 1997.

[12] To understand the discrepancies among the time series for the different LHF data sets, we examine the variations of the meteorological state variables used as the input variables in the bulk flux algorithms. Figures 2b–2d show the anomaly time series of the monthly averaged sea surface temperature (SST), wind speed (U) and air specific humidity (q_a) over the region 35°S–35°N.

[13] In Figure 2b, the time series of SST clearly show strong positive anomalies associated with the 1997/98 El Niño event. HOAPS2 shows an extreme cold SST in mid-1991, which leads to a spike in the HOAPS2 LHF. The timing of this spike suggests an inappropriate retrieval of SST in response to the eruption of Mount Pinatubo. HOAPS2 uses the NOAA/NASA Pathfinder SST data set [*Kilpatrick et al.*, 2001], whereas the other three data sets use various versions of the NOAA operational SST products [*Reynolds et al.*, 2002].

[14] Figure 2c shows small positive trends in the wind speed for each of the four data sets, with much larger intraseasonal variability. The wind speed time series for NCEP-R2 and ERA-40 track each other very closely. Significant differences are seen between the two satellite wind data sets, particularly during the period 1989–1991, where GSSTF2 is biased low relative to HOAPS2. HOAPS2 and GSSTF2 use two different versions of the SSM/I data set, applying different calibration procedures.

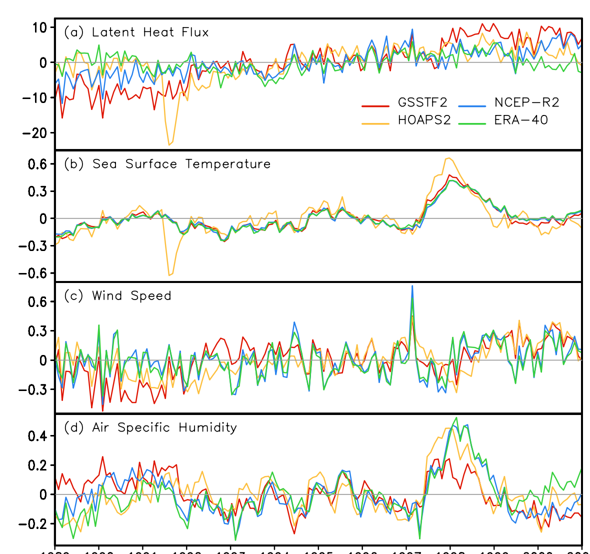

Figure 2. Anomaly time series of the monthly averaged (a) LHF (W/m^2), (b) sea surface temperature (°C), (c) wind speed (m/s), (d) air specific humidity (kg/kg) over the region 35°S–35°N.

Table 1. Trends of the LHF and Input Meteorological State Variables Over the Region 35°S–35°N[a]

Trend (per decade)	Satellite		Reanalysis	
	GSSTF2	HOAPS2	NCEP-R2	ERA-40
LHF, W/m^2	**16.80** (123.1)	**8.37** (114.5)	**8.93** (135.7)	1.64 (121.2)
SST, °C	0.18	0.19	0.19	0.21
U, m/s	**0.35**	**0.27**	**0.14**	**0.12**
q_a, kg/kg	−0.13	0.08	0.03	0.19

[a]Trends exceeding 95% confidence level are in boldface, and annual mean LHF is shown in parenthesis.

The two satellite data sets also use different wind retrieval algorithms, with GSSTF2 using *Wentz* [1997], and HOAPS2 using a neural network (http://www.hoaps.org).

[15] Figure 2d shows some substantial discrepancies among the different data sets for the air specific humidity. GSSTF2 shows substantially different variations than the other three data sets. In particular, the GSSTF2 values are biased high relative to the other data sets during the period 1989–1991, which was the same period for which a bias was noted in the GSSTF2 wind speed (Figure 2c). Again, the two satellite data sets use different humidity retrieval algorithms (with GSSTF2 using *Chou et al.* [2004], and HOAPS2 using *Bentamy et al.* [2003]), which contributes to the differences in the two satellite humidity data sets. An additional anomaly in the GSSTF2 values is seen during the 1997/98 El Niño event, where the GSSTF2 values are substantially lower than the other three data sets. It is also worth noting the divergence of the NCEP-R2 and ERA-40 time series during late 1998–2000, which is possibly associated with the assimilation of different sources of the TOVS (TIROS Operational Vertical Sounder)/ATOVS (Advanced TOVS) data by ECMWF (The TOVS/ATOVS data from October 1998 onward is taken from the ECMWF archive, rather than obtained from the NCAR, NASA and LMD archives like before October 1998 (http://www.ecmwf.int/research/era/Observations/Satellite/TOVS)).

[16] According to the bulk aerodynamic formula, larger values of the wind speed and larger difference between the saturated and air specific humidity imply larger LHF values. Apart from the spike in the HOAPS2 SST, the differences among the LHF time series are dominated by the differences in the air specific humidity.

4. Trend Analysis and Interpretation

[17] Trend analysis of the monthly averaged LHF and the input variables is performed using linear least-squares fit regression (Table 1). All trends reported as statistically significant hereafter exceed the 95% confidence level using a method that takes into account effects of the magnitude of variability and autocorrelation of the noise in the data on trend detection [*Weatherhead et al.*, 1998]. All data sets clearly show an increasing trend in the LHF over the tropical and subtropical oceans (Table 1), which is statistically significant (except ERA-40).

[18] Table 1 also shows the trends for the sea surface temperature, wind speed, and air specific humidity over the tropical and subtropical oceans. Each of the four data sets shows increasing trends for the wind speed and sea surface temperature, which contribute to the positive trend in the LHF. However, only the wind speed trends are statistically significant. By contrast, the four data sets show substantially different values for the trend in the air specific humidity (not statistically significant), which is not surprising from Figure 2d. Thus, the trend in the LHF is associated primarily with the increasing trend in the wind speed. To further enhance the reliability of the identified increase in the wind speed, we calculated the wind speed trend using the COADS data set (which is obtained from ships, buoys and other platform types). The result shows that the wind speed does have a significant positive trend (0.32 m/s per decade) over the tropical and subtropical oceans.

[19] Figure 3 shows the spatial distributions of the LHF trends. The spatial patterns of the LHF trends show general qualitative agreement across the four data sets. The LHF shows increasing trends over the trade wind belts of the eastern portions of the subtropical Pacific, the monsoon wind region of the Southeast Indian Ocean and Arabian Sea, and the western boundary current regions of the Kuroshio and Gulf Stream, and decreasing trends over the eastern equatorial Pacific and between the tropical western Pacific and Indian Ocean.

[20] The variability of the LHF is determined by the interactions of physical processes at a variety of spatial/temporal scales. The ENSO is well recognized as the dominant mode of interannual climate variability, which has strong impacts on the tropical and subtropical climate. A logical question is whether the identified positive trend in the LHF is due to the ENSO variability. The ENSO index (the Niño3 index from http://www.cdc.noaa.gov/ClimateIndices) shows a slightly negative trend for 1989–2000, and the LHF anomaly time series have insignificant correlations with the ENSO index (−0.05, −0.15, −0.08 and 0.05 for GSSTF2, HOAPS2, NCEP-R2 and ERA-40, respectively). Thus, the ENSO cannot explain the identified LHF trend.

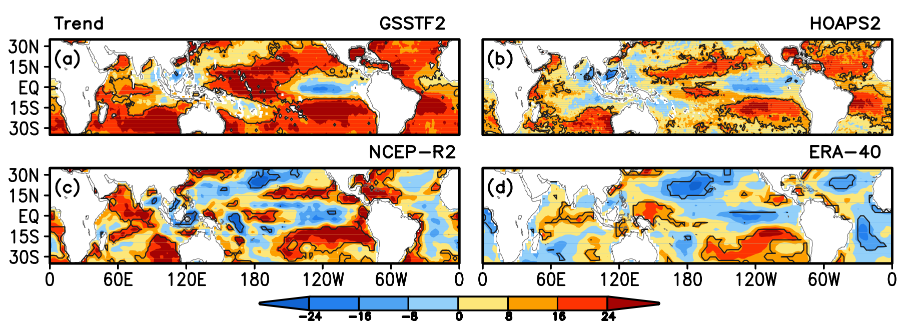

Figure 3. Spatial distributions of the LHF trends (W/m^{2}per decade) over the period 1989–2000 (Contours give the trends above 95% confidence level).

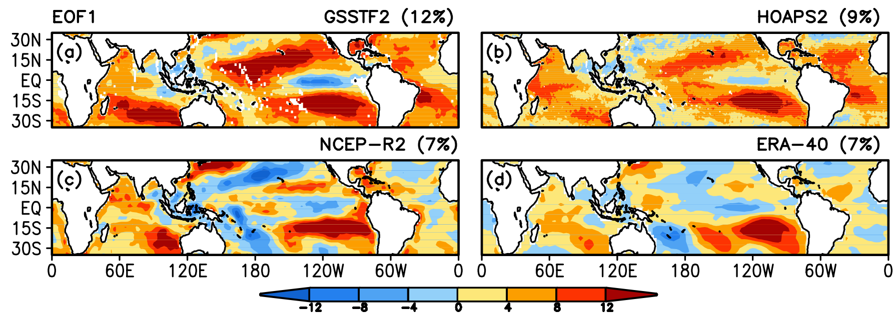

Figure 4. First EOF modes of the LHF over the period 1989–2000.

[21] The Empirical Orthogonal Function (EOF) analysis decomposes temporal variations into orthogonal spatial patterns that sometimes reveal independent physical mechanisms. When the EOF analysis is applied to the LHF anomalies after removing the impacts of the ENSO [*An*, 2003], the first EOF spatial patterns (Figure 4, they are statistically significant) resemble the spatial distributions of the LHF trends in Figure 3. Moreover, the first principal components (not shown) describing the time evolution of the first spatial patterns are strongly correlated with the LHF anomaly time series in Figure 2a (0.93, 0.87, 0.73 and 0.68 for GSSTF2, HOAPS2, NCEP-R2 and ERA-40, respectively), and also show a statistically significant increasing trend for all the data sets. This lends more confidence to the identified LHF trend, and suggests that the mechanism responsible for the trend identified here is independent of ENSO.

5. Conclusions

[22] This analysis of the ocean surface latent heat flux data sets has shown that the new versions of the satellite-based data sets (GSSTF2, HOAPS2) and two NWP reanalyses (NCEP-R2, ERA-40) show substantially more consistency among them than did the original versions of these data sets. The analysis of the input variables used to calculate LHF (sea surface temperature, surface wind, and air specific humidity) show some spurious spikes.

[23] Trend analysis was conducted on the LHF and input variables. Both the satellite-based data sets and reanalysis products showed a significant decadal-scale positive trend in the LHF. The spatial variations of the LHF trends showed reasonable consistency among the data sets, though discrepancies are observed in the subtropical central north Pacific. The ENSO was found to have little impact on the identified LHF trend, and the first principal component of the EOF analysis after removing the impacts of ENSO further supported a clear positive trend in all four of the data sets.

[24] We conclude that there is an independent decadal-scale positive trend (independent of ENSO) during the period 1989–2000 in the tropical and subtropical ocean surface heat flux, that is strongest in the Southeast Pacific and Southeast Indian subtropics. This trend in the LHF is driven primarily by the increasing trend in the surface wind speed, which might be associated with a decadal strengthening of the Hadley-Walker circulation [*Cess and Udelhofen*, 2003; C. Klepp, personal communication, 2005]. This conclusion is supported by both the satellite-based data sets and NWP reanalysis products, which are relatively independent data sources. Although there are some discrepancies among the data sets that require continued investigation, their relative consistency and the analysis of the sources of the discrepancies conducted here lends confidence to the trends identified in this study.

[25] These results have potential implications for understanding trends in the tropical and subtropical atmosphere and ocean associated with the strengthening of the Hadley-Walker circulation, and for understanding trends in hurricane frequency and intensity [*Webster et al.*, 2005].

[26] **Acknowledgments.** This research is supported by NASA NEWS. We thank Shu-Hsien Chou and Christian Klepp for information of the GSSTF2 and HOAPS2 data.

References

An, S.-I. (2003), Conditional maximum covariance analysis and its application to the tropical Indian Ocean SST and surface wind stress anomalies, *J. Clim.*, *16*, 2932–2938.

Bentamy, A., K. B. Katsaros, A. M. Mestas-Nuñez, W. M. Drennan, E. B. Forde, and H. Roquet (2003), Satellite estimates of wind speed and latent heat flux over the global oceans, *J. Clim.*, *16*, 637–656.

Cess, R. D., and P. M. Udelhofen (2003), Climate change during 1985–1999: Cloud interactions determined from satellite measurements, *Geophys. Res. Lett.*, *30*(1), 1019, doi:10.1029/2002GL016128.

Chou, S.-H., E. J. Nelkin, J. Ardizzone, and R. M. Atlas (2004), A comparison of latent heat fluxes over global oceans for four flux products, *J. Clim.*, *17*, 3973–3989.

Curry, J. A., et al. (2004), SEAFLUX, *Bull. Am. Meteorol. Soc.*, *85*, 409–424.

da Silva, A. M., C. C. Young, and S. Levitus (1994), *Atlas of Surface Marine Data*, vol. 3, *Anomalies of Heat and Momentum Fluxes*, *NOAA Atlas NESDIS 8*, 413 pp., NOAA, Silver Spring, Md.

Grassl, H., V. Jost, R. Kumar, J. Schulz, P. Bauer, and P. Schluessel (2000), The Hamburg Ocean-Atmosphere Parameters and Fluxes from Satellite Data (HOAPS): A climatological atlas of satellite-derived air-sea-interaction parameters over the oceans, *Rep. 312*, Max-Planck-Inst. for Meteorol., Hamburg, Germany.

Kanamitsu, M., W. Ebisuzaki, J. Woolen, J. Potter, and M. Fiorino (2002), NCEP/DOE AMIP-II reanalysis (R-2), *Bull. Am. Meteorol. Soc.*, *83*, 1631–1643.

Kilpatrick, K. A., G. P. Podestá, and R. Evans (2001), Overview of the NOAA/NASA advanced very high resolution radiometer Pathfinder algorithm for sea surface temperature and associated matchup database, *J. Geophys. Res.*, *106*, 9179–9197.

Kubota, M., A. Kano, H. Muramatsu, and H. Tomita (2003), Intercomparison of various surface latent heat flux fields, *J. Clim.*, *16*, 670–678.

Reynolds, R. W., N. A. Rayner, T. M. Smith, D. C. Stokes, and W. Wang (2002), An improved in situ and satellite SST analysis for climate, *J. Clim.*, *15*, 1609–1625.

Romanou, A., S. H. Chou, and W. B. Rossow (2006), Decorrelation scales of high resolution turbulent fluxes at the ocean-surface and a method to fill-in gaps in satellite data products, *J. Clim.*, in press.

Weatherhead, E. C., et al. (1998), Factors affecting the detection of trends: Statistical considerations and applications to environmental data, *J. Geophys. Res.*, *103*, 17,149–17,161.

Webster, P. J., G. J. Holland, J. A. Curry, and H.-R. Chang (2005), Changes in tropical cyclone number, duration, and intensity in a warming environment, *Science*, *309*, 1844–1846.
Wentz, F. J. (1997), A well-calibrated ocean algorithm for SSM/I, *J. Geophys. Res.*, *102*, 8703–8718.
Woodruff, S. D., S. J. Lubker, K. Wolter, S. J. Worley, and J. D. Elm (1993), Comprehensive Ocean-Atmosphere Data Set (COADS) release 1a: 1980–92, *Earth Syst. Monit.*, *4*, 4–8.
Working Group on Air-Sea Fluxes (2001), Intercomparison and validation of ocean-atmosphere energy flux fields, Final report of the joint WCRP/SCOR working group on air-sea fluxes, *WCRP Rep. 112*, 296 pp., Geneva, Switzerland.

J. A. Curry and J. Liu, School of Earth and Atmospheric Sciences, Georgia Institute of Technology, Atlanta, GA 30332, USA. (jliu@eas.gatech.edu)